Structural variability of 4f and 5f thiocyanate complexes and dissociation of uranium(III)–thiocyanate bonds with increased ionicity

Article

Accepted Version

Inorganic Chemistry

Article

Cite This: Inorg. Chem. XXXX, XXX, XXX-XXX

pubs.acs.org/IC

Structural Variability of 4f and 5f Thiocyanate Complexes and Dissociation of Uranium(III)−Thiocyanate Bonds with Increased Ionicity

Saptarshi Biswas,[†,∥] Shuwen Ma,[‡] Stefano Nuzzo,[†] Brendan Twamley,[†] Andrew T. Russell,[‡] James A. Platts,[§] František Hartl,[*,‡] and Robert J. Baker[*,†]

[†]School of Chemistry, University of Dublin, Trinity College, Dublin 2, Ireland

[‡]Department of Chemistry, University of Reading, Whiteknights, Reading RG6 6AD, U.K.

[§]School of Chemistry, Cardiff University, Main Building, Park Place, Cardiff CF10 3AT, U.K.

Supporting Information

ABSTRACT: A series of complexes $[Et_4N][Ln(NCS)_4(H_2O)_4]$ (Ln = Pr, Tb, Dy, Ho, Yb) have been structurally characterized, all showing the same structure, namely a distorted square antiprismatic coordination geometry, and the Ln−O and Ln−N bond lengths following the expected lanthanide contraction. When the counterion is Cs^+, a different structural motif is observed and the eight-coordinate complex $Cs_5[Nd(NCS)_8]$ isolated. The thorium compounds $[Me_4N]_4[Th(NCS)_7(NO_3)]$ and $[Me_4N]_4[Th(NCS)_6(NO_3)_2]$ have been characterized, and high coordination numbers are also observed. Finally, attempts to synthesize a U(III) thiocyanate compound has been unsuccessful; from the reaction mixture, a heterocycle formed by condensation of five MeCN solvent molecules, possibly promoted by U(III), was isolated and structurally characterized. To rationalize the inability to isolate U(III) thiocyanate compounds, thin-layer cyclic voltammetry and IR spectroelectrochemistry have been utilized to explore the cathodic behavior of $[Et_4N]_4[U(NCS)_8]$ and $[Et_4N][U(NCS)_5(bipy)_2]$ along with a related uranyl compound $[Et_4N]_3[UO_2(NCS)_5]$. In all examples, the reduction triggers a rapid dissociation of $[NCS]^-$ ions and decomposition. Interestingly, the oxidation chemistry of $[Et_4N]_3[UO_2(NCS)_5]$ in the presence of bipy gives the U(IV) compound $[Et_4N]_4[U(NCS)_8]$, an unusual example of a ligand-based *oxidation* triggering a metal-based *reduction*. The experimental results have been augmented by a computational investigation, concluding that the U(III)−NCS bond is more ionic than the U(IV)−NCS bond.

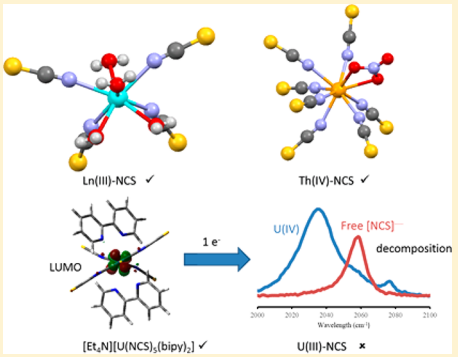

INTRODUCTION

One methodology for the treatment of legacy, current, and future nuclear waste is the partition and transmutation concept,[1] whereby the actinides (An) are separated from the lanthanide (Ln) fission products, which then undergo neutron bombardment reactions to form radioisotopes of much shorter half-lives that ease the burden on final storage. The difficult scientific challenge is separating the Ln 4f-elements from the An 5f-elements, in particular the minor actinides Am and Cm, as the 5f-orbitals drop in energy, becoming more core-like and thus resembling the lanthanides. One strategy that has seen success is by solvent extraction mechanisms, where a specifically designed ligand, most successfully 2,6-bis(5,6-dialkyl-1,2,4-triazin-3-yl)pyridines and derivatives,[2] will preferentially coordinate to the actinide over the lanthanide,[3] and some evidence for enhanced covalency in the An 5f systems has been presented.[4] Experimentally, a number of studies of U(III) and Ln(III) using N-donor ligands of varying denticity have been reported and changes in bond lengths interpreted as evidence for a more covalent U−N bond.[5] One interesting ligand type that has been investigated is the thiocyanate ion. It can be used in liquid−liquid extractions for the actinides as the stability constant for higher-order complexes $[Am(NCS)_2]^+$ is higher than that for the corresponding Eu complex (e.g., β_2 = 4.19 for Am and 1.93 for Eu).[6] [A336][SCN] (A336 = tricaprylmethylammonium) is a task-specific ionic liquid of sufficiently low viscosity to be used without utilizing a separate extractant, and substantial distribution ratio enhancements have been reported, although the mechanism is unknown.[7]

The solution-based separation data, however, do not give information on the solid state structures of the Ln or An thiocyanate compounds, and structural studies are required to verify these observations. Lanthanide thiocyanate complexes are well reported in the literature and display a rich coordination chemistry.[8] Early lanthanides favor higher coordination numbers such as 10 in $[^nBu_4N]_3[Ln(NCS)_2(NO_3)_4]$ (Ln = Ce,[9] Nd[10]), while coordination number 9 is found in [Ln(18-crown-6)$(NCS)_3$] (Ln = Eu, Tb).[11] Coordination number 8 is common in structures as diverse as $[^nBu_4N]_3[Ln(NCS)_4(NO_3)_2]$ (Ln = Nd, Dy, Yb),[12] $[Ph_3PNH_2][Sm(NCS)_4(DME)_2]$,[13] $[Me_4N]_5[Ln(NCS)_8]\cdot 2Sv$ (Ln = La, Ce,

Received: June 22, 2017

DOI: 10.1021/acs.inorgchem.7b01560
Inorg. Chem. XXXX, XXX, XXX−XXX

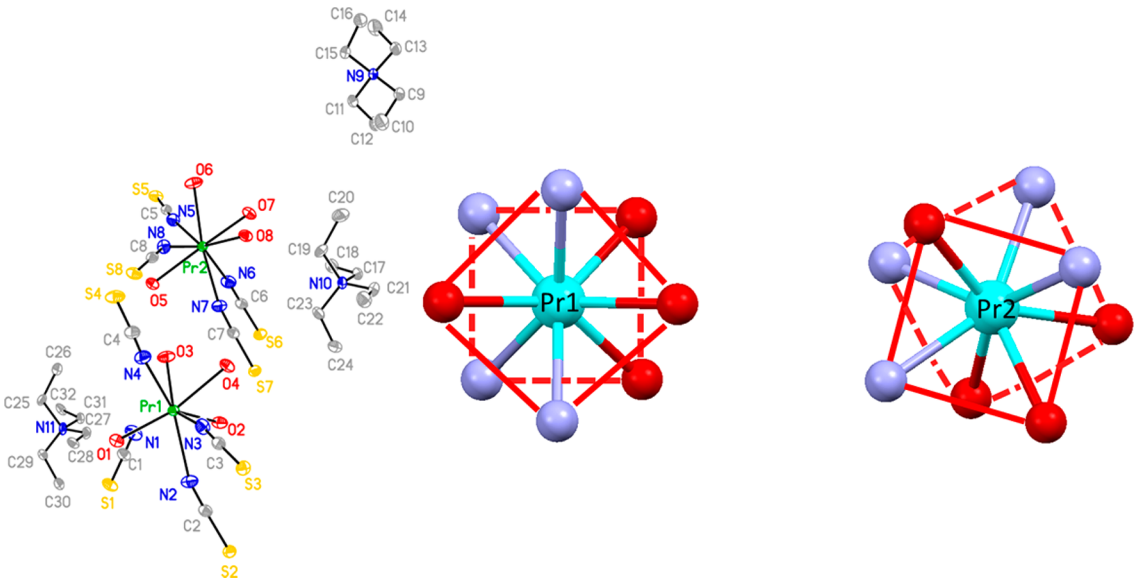

Figure 1. (left) The asymmetric unit of complex **1** with thermal displacement at 50% probability; (right) geometry around the Pr metal center. Hydrogen atoms are omitted for clarity.

Pr, Nd, Sm, Eu, Gd, Tb, and Dy; Sv = C_6H_6),[14] the ionic liquids $[Bmim]_4[Ln(NCS)_7(H_2O)]$ (Bmim = 1-butyl-3-methylimidazolium; Ln = La, Pr, Nd, Sm, Eu, Gd, Tb, Ho, Er, and Yb),[15] and $[C_6mim]_5[Dy(NCS)_8]$ (C_6mim = 1-hexyl-3-methylimidazolium),[16] $[Et_4N]_4[Ce(NCS)_7(H_2O)]$,[17] $[Et_4N]_3[La(NCS)_6(H_2O)(MeOH)]$,[18] $[Et_4N][Ln(NCS)_4(H_2O)_4]$ (Ln = Nd, Eu),[19] and $K[Ln(NCS)_4(H_2O)_4]\cdot 3KNCS\cdot 2H_2O$ (Ln = Nd, Lu).[20] Coordination numbers 7 in $[Et_4N]_4[Ln(NCS)_7]\cdot C_6H_6$ (Ln = La, Pr)[21] and 6 in $[^nBu_4N]_3[Ln(NCS)_6]$ (Ln = Y, Pr, Nd, Sm, Eu, Gd, Dy, Ho, Er, Yb, Lu)[22] or $[Et_4N]_3[Ln(NCS)_6]\cdot S$ (Ln = Er, Yb; S = aromatic solvents)[23] have also been reported. In general, these data illustrate the expected lanthanide contraction in both coordination numbers and bond lengths.

For the actinides, structurally characterized thiocyanate complexes are scarce but required for Ln/An differentiation; notably, high coordination numbers are prevalent. For example, the 10-coordinate complex $[^nBu_4N]_3[Th(NO_3)_3(NCS)_4]$,[24] eight-coordinate complexes $[Et_4N]_4[An(NCS)_8]$ (An = Th,[25] U[26] or Pu[17]) or $[Me_4N]_4[Np(NCS)_8]$[27] and the seven-coordinate geometry in $[Th(NCS)_4(DIPIBA)_4]$ (DIPIBA = ^{i}PrCON^{i}Pr$_2$)[28] are known. Throughout all the 4f and 5f compounds, structural studies have shown that the bonding is more ionic, via the harder N atom. Moreover, the M−N−C angle is much smaller than that typically seen for transition metals, which can also be attributed to the increased ionicity in the f-block compared to the d-block metals.[29] Upon coordination to the f-block metal, the N≡C and C−S bond changes only slightly, suggesting little reorganization in the π-framework of the ligand and thus only σ-bonding from the nitrogen.

We have recently reported an in-depth study of $[Et_4N]_4[An(NCS)_8]$ (An = Th, U)[30] and reinvestigated the oxidation state of the uranium center in $[Et_4N][U(NCS)_5(bipy)_2]$.[31] We now turn our attention to U(III) thiocyanate complexes that have not been reported to date, especially as $[Et_4N]_4[Pu(NCS)_8]$ was synthesized via oxidation of a Pu(III) starting material.[17] In this contribution, we present structural studies of $[Et_4N][Ln^{III}(NCS)_4(H_2O)_4]$ (Ln = Pr, Tb, Dy, Ho, Yb), $Cs_5[Nd(NCS)_8]$, and $[Me_4N]_4[Th(NCS)_7(NO_3)]$, along with unsuccessful attempts to stabilize and isolate chemically reduced U(III) thiocyanate complexes. Thin-layer cyclic voltammetry and IR spectroelectrochemistry were employed to explore the redox behavior of U(IV) and related U(VI) compounds in more detail. The experimental work is supported by a computational study on the putative homoleptic U(III) compound.

RESULTS AND DISCUSSION

Lanthanide Structural Studies. In our experiments, we used a two solvent system to grow single crystals and reproducibly isolated $[Et_4N][Ln(NCS)_4(H_2O)_4]$ {Ln = Pr (**1**), Tb (**2**), Dy (**3**), Ho (**4**), Yb (**5**)} rather than hepta- or octathiocyanate complexes; presumably, this is due to the intrinsic ionic nature of the bonding and the excess of water present. The structure of **1** is shown in Figure 1, while **2**−**5** are in the Supporting Information, Figures S1−S4; pertinent bond lengths are collated in Table 1 and Supporting Information,

Table 1. Selected Geometric and Spectoscopic Data for 1−5 and Related Lanthanide Compounds

lanthanide	average Ln−N (Å)	average Ln−O (Å)	ref
Pr (**1**)	2.525(2)	2.481(2)	this work
Nd	2.500(9)	2.473(8)	19
Eu	2.4556(10)	2.421(10)	19
Tb (**2**)	2.436(3)	2.392 (3)	this work
Dy (**3**)	2.428(5)	2.385(4)	this work
Ho (**4**)	2.412(2)	2.369(2)	this work
Yb (**5**)	2.394(2)	2.360(3)	this work
Lu[a]	2.3309(17)	2.4086(15)	20

[a]The geometry of $[Lu(NCS)_4(H_2O)_4]^-$ has an all *trans* arrangement, whereas all others are *cis* and *trans*.

Table S1. The asymmetric unit contains two eight-coordinate lanthanide ions surrounded by four thiocyanato anions and four coordinated water molecules in a distorted square antiprismatic environment; there are no significant differences in the metric parameters between the two molecules. The average metal−nitrogen and metal−oxygen bond distances decrease with the increasing atomic number of the metal ion, as expected, while

DOI: 10.1021/acs.inorgchem.7b01560
Inorg. Chem. XXXX, XXX, XXX−XXX

the average Ln−O distances are shorter than the average Ln−N bond distances. The N≡C and C−S bond lengths are the same as those found in the related uranium compounds.[30] Given that Nd and Eu analogues $[Et_4N][Ln(NCS)_4(H_2O)_4]$[19] and a similar lutetium complex,[20] $K[Ln(NCS)_4(H_2O)_4]\cdot 3KNCS\cdot 2H_2O$, have been structurally characterized, we can compare the bond lengths through the series (Table 1) and show that the lanthanide contraction is indeed evident in these compounds. However, it is worth noting that the Lu example has a different arrangement of the ligands so that two water molecules and two thiocyanato ligands are *trans* in the square of the square antiprism, while all other compounds have a *trans* and *cis* arrangement; this influences the Ln−O bond length the most.

Notably, the hydrogen atoms on the coordinated water molecules in **1**−**5** are involved in hydrogen bonding to the sulfur atom of an $[NCS]^-$ ion. The S···O distances range 3.208(2)−3.288(2) Å and in line with other examples of this weak hydrogen bonding in the literature.[32]

If the counterion is changed from Et_4N^+ to Cs^+, a different structural motif is observed and the coordination polymer $Cs_5[Nd(NCS)_8]$ (**6**) isolated in the same solvent mixture as for **1**−**5**. The structure is shown in Figure 2. The geometry at the

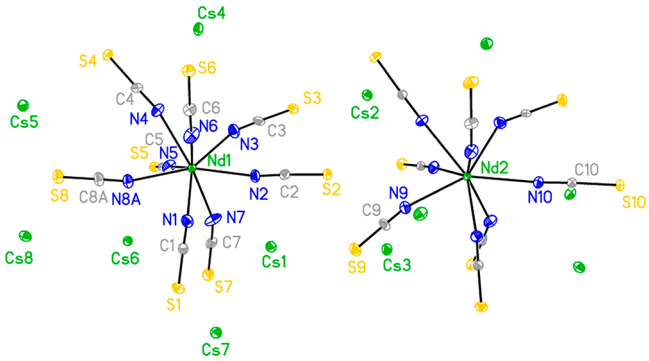

Figure 2. Molecular structure of **6**. Thermal displacement at 50% probability. Selected bond lengths (Å) and angles (deg): Nd(1)−N(1) 2.564(8); Nd(1)−N(2) 2.570(7); Nd(1)−N(3) 2.516(8); Nd(1)−N(4) 2.573(7); Nd(1)−N(5) 2.551(7); Nd(1)−N(6) 2.519(7); Nd(1)−N(7) 2.511(8); Nd(1)−N(8) 2.498(19); Nd(1)−N(8A) 2.498(15).

Nd center is intermediate between a cube and square antiprism, while the Nd−N bond lengths are in the range 2.498(19)−2.573(7) Å that is very similar to $[Et_4N][Nd(NCS)_4(H_2O)_4]$.[19] The structure features numerous Cs···E (E = N, C, S) contacts that give a complex packing arrangement as shown in Figure 3.

All the complexes have also been characterized by IR and Raman spectroscopy (Supporting Information, Figures S6, S7), as the number of N≡C stretches is diagnostic of the geometry. Thus, for a square antiprismatic symmetry, three Raman-active ν(C≡N) stretches ($A_1 + E_2 + E_3$) and two IR stretches ($B_2 + E_1$) are expected. In **1**−**5**, three bands are observed at ca. 2115, 2090, and 2080 cm^{-1} in the Raman spectra. In the infrared spectra, only a broad peak is observed, but the shift in frequency of the C≡N bond stretch is in keeping with the change in the size of the lanthanide ion, as has been noted previously.[20] Dissociation of $[NCS]^-$ was not observed, as revealed by the absence of the band at 2060 cm^{-1}. For **6**, two bands are evident in the IR spectrum, and the Raman spectrum shows two bands at 2063 and 2052 cm^{-1} (Table 2).

Actinide Structural Studies. In comparison to the lanthanides, actinide thiocyanate compounds are much rarer. To expand the library of these compounds, we have prepared some thorium compounds. Thus, the reaction of $Th(NO_3)_4$ with 8 equiv of NaNCS and 4 equiv of Me_4NCl in MeCN reproducibly afforded the nine-coordinate mixed ligand species $[Me_4N]_4[Th(NCS)_7(NO_3)]\cdot 2MeCN$, **7**; the structure is shown in Figure 4. Upon repeating this synthesis, we also obtained a structure that was disordered, and it was possible, with some restraints, to refine this to 95% of 7.2MeCN and 5% of $[Me_4N]_4[Th(NCS)_6(NO_3)_2]\cdot 2MeCN$, **8**. The structure of **8** is shown in Figure 5. With caution, we can compare the structural parameters with those known for $[^nBu_4N]_3[Th(NO_3)_3(NCS)_3]$. The average Th−N and Th−O bond lengths are essentially invariant as are the N≡C and C−S bond lengths, consistent with the ionic bonding of these ligands. The infrared spectrum of **7** show bands associated with the nitrate at 1480 cm^{-1} and the ν(N≡C) at 2041 cm^{-1}.

Our attempts to synthesize a U(III) thiocyanate complex have not been successful. Reaction of $[UCl_3(py)_4]$ (ref 33) at −78 °C or the reduction of $[Et_4N]_4[U(NCS)_8]$ with a variety of reducing agents, such as Na/Hg, K, or $NaC_{10}H_8$, repeatedly failed to give any isolable uranium thiocyanate compounds. We have tried to follow the reduction with UV−vis spectroscopy in a cuvette. Upon addition of the reagents, an immediate precipitate is formed and all color bleaches from the solution. In a Schlenk flask at −78 °C, we also see the same effect and the solid produced shows no N=C stretches in the IR spectrum. However, with the reducing agent being KC_8 in MeCN, a few colorless single crystals were isolated, and this was shown to be heterocycle **9** (Figure 6), formed by condensation of five MeCN molecules. The mechanism of the formation of this unusual byproduct is discussed further in Supporting Information (Scheme S1), although it is worth noting that U(IV) amides trimerizes MeCN,[34] while the Lewis acidic U(III) ion has been known to cleave THF[35] and Et_2O[36] and reductively couple MeCN.[37] While it could be possible that U(III) rapidly reduces $[NCS]^-$, this is unlikely as free thiocyanate can be used as a reducing agent[38] but complexed thiocyanate is readily oxidized to the corresponding radical.[30]

The 2,2′-bipyridine (bipy) ligand is well-known to be redox active,[39] and several actinide complexes have been reported in the formal metal(III),[40] metal(IV),[41] and inconclusive[42] oxidation states and with singly or doubly reduced bipy ligands. We therefore attempted the reduction of $[Et_4N][U(NCS)_5(bipy)_2]$ with alkali metal reducing agents in an effort to generate complexes with either a U(III) ion or U(IV) coordinated by a reduced bipy (radical anion). However, no isolable uranium compounds were obtained in any solvent used and free neutral bipy was the only species identified by ^1H NMR spectroscopy.

Spectroelectrochemical Studies on Uranium Compounds. Intrigued by the inability to isolate any chemically reduced U(III) compounds, we turned to a study of the cathodic behavior of $[Et_4N]_4[U(NCS)_8]$ using spectroelectrochemistry; our previous work focused mainly upon the oxidation of this species.[30] It must be stressed that the cathodic responses of this family of U−NCS complexes are strongly affected by adsorption and electrode passivation. The cathodic potentials read from TLCV are reliable, as the electron transfer can directly be identified by the corresponding infrared spectral changes observed during the electrolyses; we have taken advantage of this to accurately determine the potential of the

DOI: 10.1021/acs.inorgchem.7b01560
Inorg. Chem. XXXX, XXX, XXX−XXX

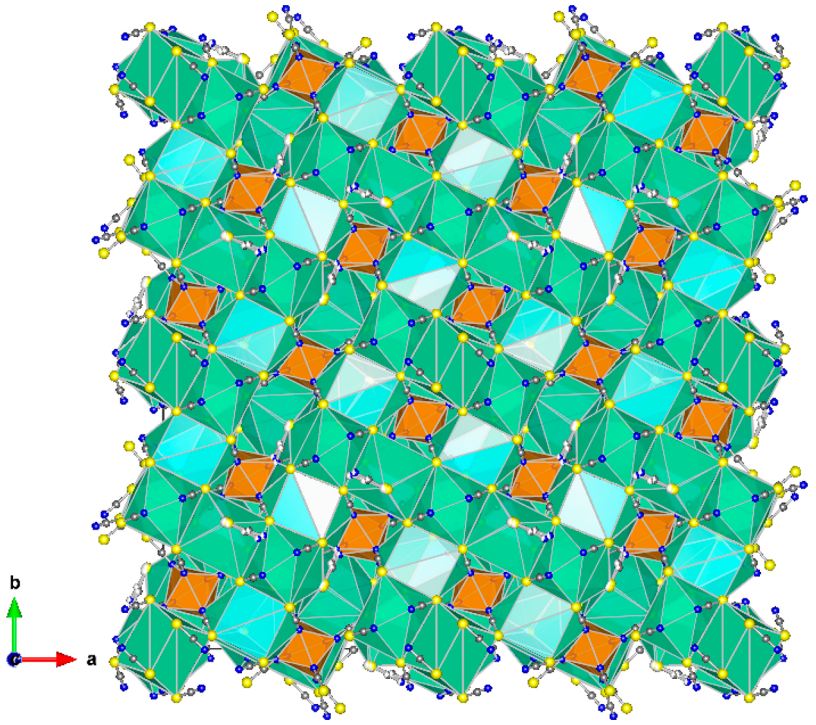

Figure 3. Packing of **6** along the crystallographic *c*-axis. Green polyhedral = Cs^+; orange = Nd^{3+}.

Table 2. Selected Vibrational Spectral Data for 1−6, Measured in the Solid State

	IR (cm^{-1})		Raman (cm^{-1})	
complex	ν(C≡N)	ν(O−H)	ν(C≡N)	ν(N−S)
1	2049(br)	3325(br)	2082, 2085, 2103	421
2	2086(br)	3310(br)	2090, 2096, 2114	420
3	2085(br)	3313(br)	2092, 2098, 2114	412
4	2087(br)	3320(br)	2092, 2097, 2116	420
5	2090(br)	3310(br)	2098, 2102, 2121	420
6	2078(br), 2114 (m)		2063, 2052	410

broad, poorly defined cathodic peak ($E_{p,c}$ = −1.80 V vs Fc/Fc^+) from conventional CV measurements.[30] To further evaluate the use of TLCV, we have also examined $[Et_4N][U(NCS)_5(bipy)_2]$ and the uranyl compound $[Et_4N][UO_2(NCS)_5]$, which also show broad CV responses due to slow reaction kinetics and/or limited by the solubility of electrochemically produced species.

The thin-layer cyclic voltammogram of $[Et_4N]_4[U(NCS)_8]$ is shown in Figure 7, and the reduction potential is $E_{p,c}$ = −1.38 V vs Fc/Fc^+. This is much less negative than that originally obtained from the conventional CV measurements ($E_{p,c}$ = −1.80 V),[30] which in light of the TLCV experiment is erroneous. During the reduction of $[Et_4N]_4[U(NCS)_8]$, the broad parent ν(C≡N) band at 2048 cm^{-1} decreases in intensity and a new peak rises at 2059 cm^{-1}, which can be assigned to free $[NCS]^-$.[43] We have recently reported a spectroelectrochemical study of Na[NCS] under the same experimental conditions,[30] which conclusively demonstrates the identity of this species. U^{III}−NCS compounds could be coincident with the free $[NCS]^-$ ion, but a different line shape would be expected. Apparently, the addition of one electron triggers dissociation of all π-donor thiocyanate ligands and decomposition of the compound. Guided by this result, we repeated the chemical reduction of the U(IV) compound in the presence of excess NaNCS but failed again to isolate any U−NCS containing product. It is clear that the thiocyanate ion does not stabilize the lower oxidation state of uranium effectively.

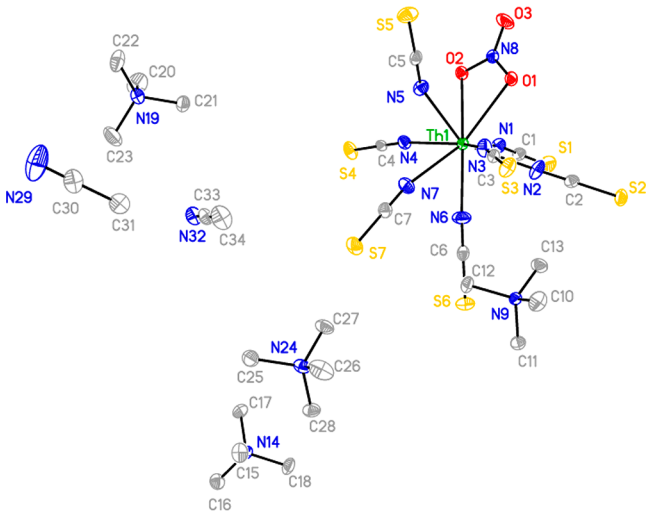

Figure 4. Asymmetric unit of **7** with atomic displacement shown at 50% probability. Hydrogen atoms omitted for clarity. Selected bond lengths (Å) and angles (deg): Th(1)−N(1) 2.5270(19); Th(1)−N(2) 2.503(2); Th(1)−N(3) 2.5360(19); Th(1)−N(4) 2.4813(18); Th(1)−N(5) 2.4841(19); Th(1)−N(6) 2.497(2); Th(1)−N(7) 2.5025(19); Th(1)−N(8) 3.0167(18); Th(1)−O(1) 2.5584(15); Th(1)−O(2) 2.6116(15); O(1)−N(8) 1.280(2); O(2)−N(8) 1.260(2); O(3)−N(8) 1.220(2); N(1)−Th(1)−O(1) 79.49(6); O(1)−Th(1)−O(2) 49.37(5); N(8)−O(1)−Th(1) 98.06(11); N(8)−O(2)−Th(1) 96.04(11); O(2)−N(8)−O(1) 116.52(17).

We next looked at the redox processes of $[Et_4N][U(NCS)_5(bipy)_2]$, as the π-acceptor bipy ligand may allow for the isolation of a stable U(III) compound or become reduced itself. Under the TLCV conditions (Figure 8), there is a clearly

DOI: 10.1021/acs.inorgchem.7b01560
Inorg. Chem. XXXX, XXX, XXX−XXX

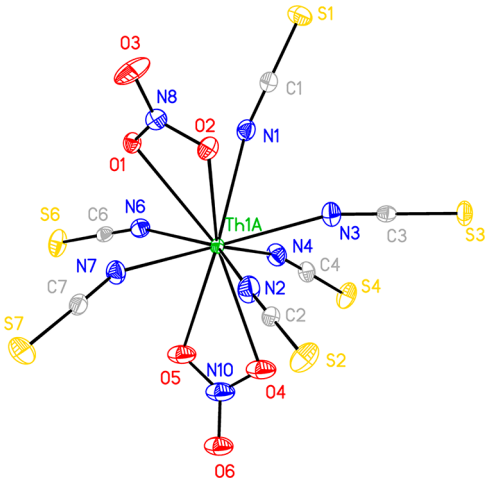

Figure 5. Disordered anionic component of **8** (5% occupied). Atomic displacement shown at 50% probability. Hydrogen atoms omitted for clarity. Selected bond lengths (Å) and angles (deg): Th(1A)−O(1) 2.875(4); Th(1A)−O(2) 2.802(4); Th(1A)−O(4) 2.812(9); Th(1A)−O(5) 2.811(9); Th(1A)−N(1) 2.762(4); Th(1A)−N(2) 2.373(5); Th(1A)−N(3) 2.572(5); Th(1A)−N(4) 2.418(5); Th(1A)−N(6) 2.523(5); Th(1A)−N(7) 2.477(5); O(1)−N(8) 1.267(3); O(2)−N(8) 1.279(3); O(3)−N(8) 1.219(3); O(4)−N(10) 1.2658; O(5)−N(10) 1.2795; O(6)−N(10) 1.2196; O(2)−Th(1A)−O(1) 44.72(7); O(5)−Th(1A)−O(4) 45.21(13); N(1)−Th(1A)−O(1) 60.19(9); N(1)−Th(1A)−O(2) 65.24(10); N(1)−Th(1A)−O(4) 143.0(8); N(1)−Th(1A)−O(5) 136.2(7); N(2)−Th(1A)−O(1) 106.22(17); N(2)−Th(1A)−O(2) 69.62(13); N(2)−Th(1A)−O(4) 62.8(7); N(2)−Th(1A)−O(5) 98.3(6).

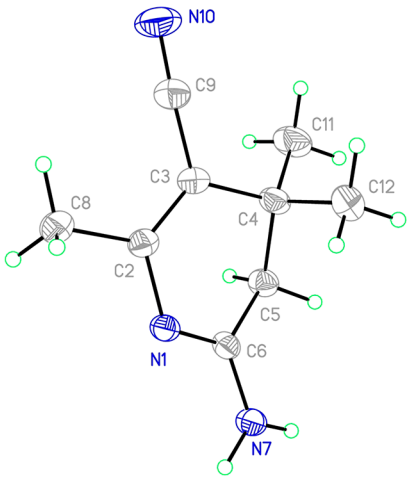

Figure 6. X-ray structure of **9** with displacement ellipsoids at 50%. Selected bond lengths (Å) and angles (deg): N1−C2 1.3861(12); N1−C6 1.3170(13); C2−C3 1.3609(14); C3−C9 1.4230(14); C3−C4 1.5240(14); C4−C5 1.5326(14); C5−C6 1.5022(13); C6−N7 1.3230(13); C9−N10 1.1518(15); N7−H7B 0.895(14); N7−H7A 0.935(15), C6−N1−C2 117.62(8); C2−C3−C4 121.02(9); C3−C4−C5 106.34(8); C4−C5−C6 111.63(8); C5−C6−N1 122.12(9).

defined reduction step at $E_{p,c}$ = −0.80 V (vs Fc/Fc^+). Because of the coordination of the π-acceptor bipy ligand, the reduction potential is significantly less negative compared to homoleptic $[U(NCS)_8]^{4-}$. IR spectroscopy shows that upon the reduction the parent bands at 2036 and 2077 cm^{-1} are replaced by a new band at 2059 cm^{-1}, again indicating free $[NCS]^-$ and decomposition of the putative U(III) compound. Interestingly, upon monitoring the one-electron oxidation of $[Et_4N][U(NCS)_5(bipy)_2]$, the IR spectra reveal the loss of the withdrawing bipy ligands, as judged from the appearance the $\nu(C{\equiv}N)$ band at 2048 cm^{-1} belonging to $[Et_4N]_4[U(NCS)_8]$ (cf. Figure 7). As expected, the coordination of the bipy ligand weakens significantly upon the oxidation. The formation of $[Et_4N]_4[U(NCS)_8]$ is also in line with the slightly more positive oxidation potential of this complex ($E_{p,a}$ = +0.24 V) compared to parent $[Et_4N][U(NCS)_5(bipy)_2]$ ($E_{p,a}$ = +0.22 V).

Finally, we examined the redox behavior of $[Et_4N]_3[UO_2(NCS)_5]$ in the presence of excess bipy. The reduction of the parent compound studied by TLCV and FT-IR (Supporting Information, Figure S12) shows a cathodic wave at $E_{p,c}$ = −1.43 V and liberation of free $[NCS]^-$, consistent with our earlier study. We have previously reported that the oxidation of the parent uranyl compound is difficult to study by cyclic voltammetry.[30] Corresponding TLCV shows irreversible oxidation at $E_{p,a}$ = +0.21 V (Supporting Information, Figure S12, right) that must be NCS-based; IR spectroelectrochemical monitoring proves the decomposition and only yellow deposits of $[NCS]_x$ are observed in the spectroelectrochemical cell. However, in the presence of bipy, a new species with a $\nu(C{\equiv}N)$ band at 2036 cm^{-1} is initially generated (Supporting Information, Figure S13, left), belonging to the uranium(IV) complex, $[U(NCS)_5(bipy)_2]^-$. Under further oxidation, the intermediate band decays and is replaced by the $\nu(C{\equiv}N)$ band of $[U(NCS)_8]^{4-}$ at 2048 cm^{-1} (Supporting Information, Figure S13), indicating that the bipy ligands dissociate (vide supra). It is interesting that a ligand-based oxidation triggers a metal-based reduction, U(VI) → U(IV). It is well-known[44] that the transient one-electron oxidized $[U(V)O_2]^+$ species undergo a disproportionation reaction to form $[U(IV)O_2]$ and $[U(VI)O_2]^{2+}$. Table 3 summarizes the redox potentials of the three uranium thiocyanate complexes measured by TLCV.

Given that the electrochemical deoxygenation is facile, we explored chemical oxidation of $[Et_4N]_3[UO_2(NCS)_5]$. Reaction with organic oxidants gave no reaction, as judged by IR and UV−vis spectroscopy. Addition of $CuCl_2$ in MeCN afforded a brown solution; however, there were no bands in the UV−vis/NIR spectral region attributable to f−f transitions. Recrystallization afforded three different morphologies of single crystals. X-ray crystallography showed these to be copper sulfate, $[Et_4N]_2[UO_2Cl_4]$, and $[Et_4N]_4[UO_2Cl_4][CuCl_4]$, **10**. Copper sulfate must have been formed from the oxidation of the $[NCS]^-$ ion,[45] as the $CuCl_2$ was sulfate-free (via IR spectroscopy). The formation of uranyl halides corroborates the results of computational investigations showing the U−Cl bond to be more covalent than the U−NCS bond.[30] The structure of **10** is unremarkable and included in the Supporting Information (Figure S14, Table S3), along with luminescence (Figure S15) and vibrational (Figures S16 and S17) data.

Computational Studies. To understand the change in reactivity between U(III) and U(IV), we turned to computational chemistry. In our previous work, we benchmarked hybrid and pure DFT methods to the vibrational data of the U(IV) compound and found that the BP86 functional gave a satisfactory fit to the experimental data.[30] We have therefore used this to compare the bonding in $[M(NCS)_8]^{5-}$, where M = Ce and U, and used QTAIM to further probe this. It is worth reemphasizing that the eight-coordinate Ce(III) compound is not known experimentally but used strictly as a comparison to U(III). Natural bond order (NBO) analysis finds a single bonding orbital for each M−N bond and indicates a charge on

DOI: 10.1021/acs.inorgchem.7b01560
Inorg. Chem. XXXX, XXX, XXX−XXX

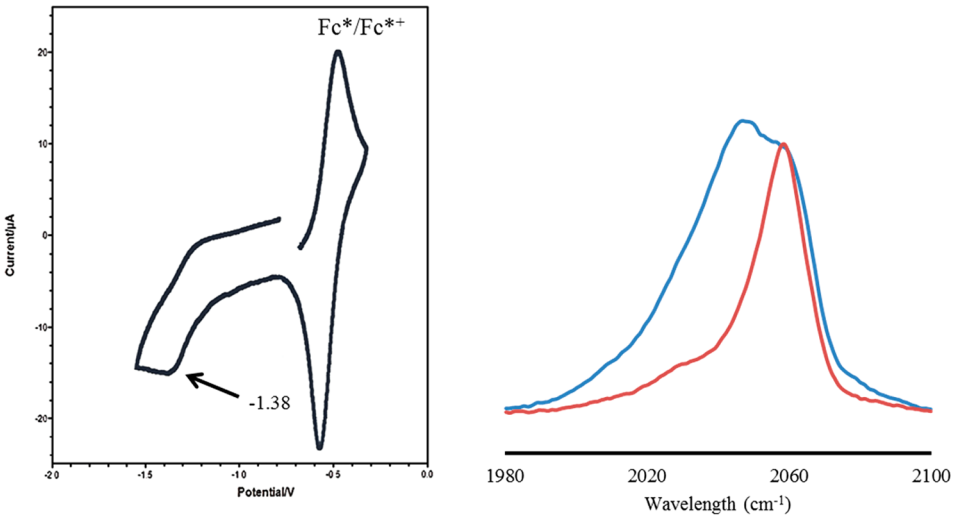

Figure 7. Left: Thin-layer cyclic voltammogram of $[Et_4N]_4[U(NCS)_8]$ against Fc/Fc^+ determined in MeCN at 293 K, with ~0.1 M Bu_4NPF_6 as the supporting electrolyte, at ν = 2 mV s^{-1}. (The depicted scan shows oxidation of decamethylferrocene, Fc^*/Fc^{*+}, used as the internal standard; two cycles were applied to exclude any potential drift.) Right: IR spectral changes in the ν(C≡N) region accompanying the one-electron reduction of $[Et_4N]_4[U(NCS)_8]$ in MeCN/Bu_4NPF_6 at 293 K within an OTTLE cell. Blue spectrum, before the reduction at −1.38 V vs Fc/Fc^+; red spectrum, after the reduction.

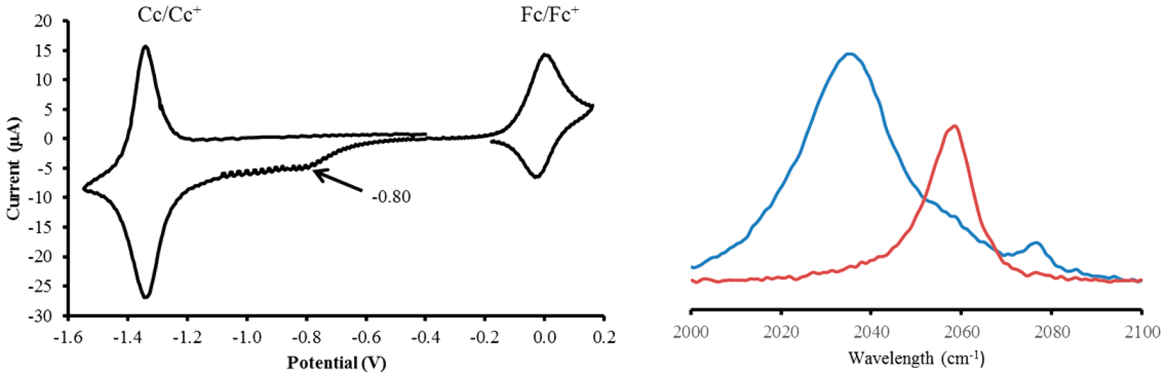

Figure 8. Left: thin-layer cyclic voltammogram of $[Et_4N][U(NCS)_5(bipy)_2]$ against Fc/Fc^+ (used as the internal standard, together with cobaltocenium, Cc/Cc^+) recorded in MeCN at 293 K, with ~0.1 M Bu_4NPF_6 as the supporting electrolyte (ν = 2 mV s^{-1}). Right: IR spectral changes in the ν(C≡N) region accompanying the 1e− reduction of $[Et_4N][U(NCS)_5(bipy)_2]$ in MeCN/Bu_4NPF_6 at 293 K within an OTTLE cell. Blue spectrum, before the reduction; red spectrum, after the reduction.

Table 3. Formal Redox Potentials of the Studied Uranium Thiocyanate Complexes against Ferrocene/Ferrocenium, Determined by Thin-Layer Cyclic Voltammetry within an OTTLE Cell[a]

complex	$E_{p,c}$ (V) (vs Fc/Fc^+)	$E_{p,a}$ (V) (vs Fc/Fc^+)
$[U(NCS)_8]^{4-}$	−1.38	0.24
$[U(NCS)_5(bipy)_2]^-$	−0.80	0.22
$[UO_2(NCS)_5]^{3-}$	−1.43	0.21

[a]In MeCN/TBAH at 293 K.

U of just +0.96 and Ce of +0.90, much less than the formal charge of +3. Inspection of the spin densities (Supporting Information, Figure S10) shows that there is a small amount of delocalization onto the NCS ligands in the U(III) compound, which is not observed in the Ce(III) species. QTAIM analysis show that both U(III) and Ce(III) are more ionic than the U(IV) compound, with a low ρ associated with the M−N bond and a decrease in the bond order (Table 4). Literature precedent exists where An−Cl have been described as showing enhanced covalency of the U(IV)−Cl bond versus the U(III)−

Table 4. DFT Geometry and Vibrational Modes Using BP86 Functional and Selected QTAIM Properties for $[U(NCS)_8]^{4-}$ and the Putative $[M(NCS)_8]^{5-}$ Compounds and Experimental (exp) Data

property	U(IV) exp	U(IV) BP86	U(III) BP86	Ce(III) BP86
M−N (Å)	2.38(3)	2.469	2.615	2.672
	2.46(3)			
N≡C (Å)	1.15(4)	1.185	1.183	1.182
	1.14(4)			
C−S (Å)	1.63(4)	1.644	1.663	1.663
	1.61(3)			
ν(C≡N) (cm^{-1})[a]	2047	2067 (b_2)	2078	2081
	2090	2071 (e_1)		
ν(C−S) (cm^{-1})[a]	783	797	748	749
ρ_{M-N} (au)		0.056	0.034	0.031
$\rho_{N\equiv C}$ (au)		0.450	0.452	0.441
ρ_{C-S} (au)		0.212	0.207	0.208
M−N bond order		0.336	0.235	0.188

[a]IR active bands.

DOI: 10.1021/acs.inorgchem.7b01560
Inorg. Chem. XXXX, XXX, XXX−XXX

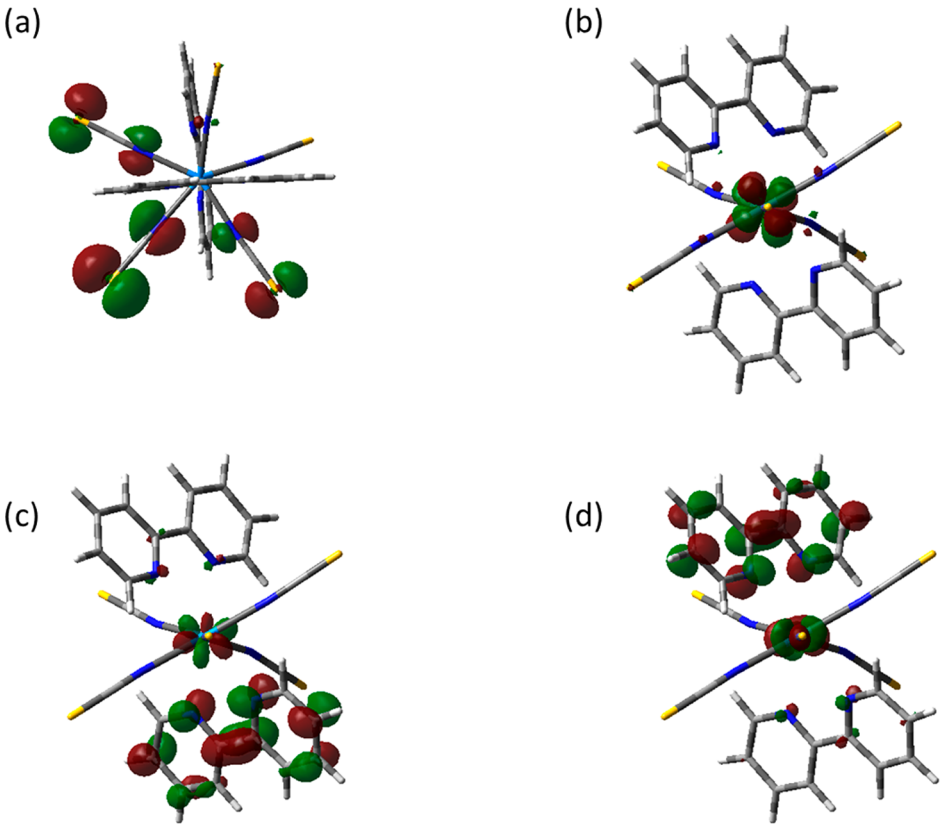

Figure 9. (a) HOMO; (b) LUMO; (c) LUMO+3; (d) LUMO+4 of $[U(NCS)_5(bipy)_2]^-$.

Cl bond.[46] Using QTAIM,[47] the ρ_{BCP} for the U−Cl bond in $[UCl_6]^{n-}$ at the B3LYP functional are 0.064 for U(IV) and 0.037 for U(III), which follows the trend in our data. In this work, the authors ascribe this partly to an increase in the localization of the f-orbitals with decreased oxidation state, which may indicate a decrease in the covalency of these bonds. This is an example of an energy mismatch between the metal and ligand orbitals in lower oxidation states. NBO analysis of the $[U(NCS)_8]^{n-}$ gives some evidence for this, as there is a decrease in the f-orbital contribution to the bonding {U(III) 11% U: made up of s (12%), p (34%), d (39%), and f (15%); U(IV) 14% U: made up of s (12%), p (33%), d (31%), and f (24%)}. We note that the U(III)−N bond is slightly less ionic than the Ce(III)−N bond and consistent with previous experimental results.[5]

The cathodic electrochemistry of $[U(NCS)_5(bipy)_2]^-$ and $[U(NCS)_8]^{4-}$ (Table 3) shows that the LUMO is stabilized by the coordination of the bipy, suggesting its participation in the electrochemical reduction. We have reinvestigated[33] $[U(NCS)_5(bipy)_2]^-$ by using tighter SCF criteria within DFT calculations and found that the LUMO is metal-based while the HOMO is based on the NCS ligands. The LUMO+3 and LUMO+4 are the lowest-lying unoccupied orbitals containing substantial contributions from π^*(bipy) combinations, as shown in Figure 9.

CONCLUSIONS

We have prepared and characterized a series of lanthanide thiocyanate complexes of the formulation $[Et_4N][Ln(NCS)_4(H_2O)_4]$ (Ln = Pr, Tb, Dy, Ho, Yb) and an unusual eight-coordinate complex $Cs_5[Nd(NCS)_8]$. For thorium chemistry, we have found that full substitution of the nitrate ions in $Th(NO_3)_4$ is difficult to achieve when using the Me_4N^+ counterion. Both mono- and bis-nitrate compounds of thorium thiocyanates were characterized by X-ray diffraction. We have attempted to prepare the homoleptic U(III) compound but under all conditions failed to isolate a metal-based species. Thin-layer cyclic voltammetry and spectroelectrochemistry have shown that this is due to the facile loss of all thiocyanate ligands upon the reduction. Theoretical approaches have reveal increased ionicity of the U(III)−N bond compared to the U(IV)−N bond. The oxidation potentials of the three studied uranium thiocyanate complexes are very similar. $[U(NCS)_8]^{4-}$ has the most positive oxidation potential because of the eight strongly π-donating $[NCS]^-$ ligands stabilizing the complex. The reduction potential of $[U(NCS)_5(bipy)_2]^-$ is much less negative than that of $[U(NCS)_8]^{4-}$ because the withdrawing 2,2′-bipyridine ligands stabilize the metallic frontier molecular orbitals. Finally, the electrochemical oxidation of $[UO_2(NCS)_5]^{3-}$ in the presence of bipy affords $[U(NCS)_8]^{4-}$ via $[U(NCS)_5(bipy)_2]^-$; however, chemical oxidation with $CuCl_2$ affords only uranyl chlorides.

EXPERIMENTAL SECTION

Caution! Natural uranium and thorium were used during the course of the experimental work. As well as the radiological hazards, uranium and thorium are toxic metals and care should be taken with all manipulations. Experiments using radioactive materials were carried out using pre-set radiological safety precautions in accordance with the local rules of the Trinity College Dublin and the University of Reading.

All manipulations for actinide chemistry were carried out using standard Schlenk and glovebox techniques under an atmosphere of a high purity dry argon. Lanthanide chemistry was conducted in air. Standard IR spectra were recorded on a PerkinElmer Spectrum One

DOI: 10.1021/acs.inorgchem.7b01560
Inorg. Chem. XXXX, XXX, XXX−XXX

spectrometer with an attenuated total reflectance (ATR) accessory. Raman spectra were obtained using 785 nm excitation on a Renishaw 1000 micro-Raman system in sealed capillaries. UV−vis/NIR measurements were conducted on a PerkinElmer Lambda 1050 spectrophotometer over the range 300−1300 nm, using fused silica cells with an optical path length of 1 cm. X-ray data were collected on a Bruker APEX DUO (**1**, **3**, and **9**) and a D8 Quest ECO (**2**, **4**−**8**) using Mo Kα radiation (λ = 0.71073 Å). Each sample was mounted on a Mitegen cryoloop and data collected using a Cobra and Oxford Cryostream cryosystem. Bruker APEX software[48] was used to collect and reduce data and determine the space group. Structures were solved using XT[49] and refined using the XL[50] program within the Olex2 program.[51] Absorption corrections were applied using SADABS 2014.[52] Details of the crystal data and refinements are given in Supporting Information, Table S2. CCDC 1554951−1554959 and 1574079 contain the supplementary crystallographic data for this paper. These data can be obtained free of charge from The Cambridge Crystallographic Data Centre via www.ccdc.cam.ac.uk/data_request/cif. The packing diagram shown in Figure 3 was generated using VESTA version 3.3.9.[53] Phase purity was checked by powder X-ray diffraction (Supporting Information, Figure S5), which was carried out on a Bruker D2 Phaser.

Cyclic voltammetric measurements were conducted with a Metrohm Autolab PGSTAT302N potentiostat in an airtight three electrode cell connected to a Schlenk line with a Pt microdisc (0.14 mm^2) working electrode, Pt coil counter electrode, and Ag coil pseudoreference electrode; the $[^nBu_4N][PF_6]$ electrolyte was recrystallized twice from absolute ethanol and dried under vacuum at 80 °C overnight. Controlled-potential electrolyses within the room-temperature OTTLE cell[54] were carried out using an EmStat3 (PalmSens) potentiostat. IR and UV/vis spectral monitoring of the redox reactions was carried out with a Bruker Vertex 70v FT-IR spectrometer and a Scinco S3100 diode array spectrophotometer, respectively. The different redox steps were localized with the aid of contemporarily recorded thin-layer cyclic voltammograms. Ferrocene, decamethylferrocene (Fc*), and cobaltocenium (Cc) were used as multiple internal potential standards in this experiment. The correct position of the cathodic response of the cobaltocenium standard (−1.34 V vs Fc/Fc^+) proves that the potential scale remained correct during the slow (2 mV s^{-1}) scan, and no potential drift occurred. For cyclic voltammetry and IR spectroelectrochemistry analysis, the compounds were first characterized by IR spectroscopy (Supporting Information, Table S2). The uranium complexes were dissolved in dry acetonitrile containing the supporting electrolyte and checked for decomposition.

DFT geometry optimization was performed on single molecules extracted from the crystal structure at the unrestricted BP86/def2-TZVP[55,56] level using Turbomole[57] initially without symmetry constraints but subsequently in the D_{4d} point group. Scalar relativistic effects in uranium were included through the use of effective core potentials, as defined for this basis set. Spin contamination was not significant, with values of S^2 within 1% of the anticipated value of 2.00. Further single-point DFT calculations were performed in Gaussian09[58] using the BP86 and B3LYP[59] functionals. The (27s 24p 18d 14f 6g)/[8s 7p 5d 3f 1g] all-electron ANO-RCC basis sets of DZP quality were used for uranium,[60] with 6-31+G(d,p) on C, N, and S.[61] Scalar relativistic effects were included via the second-order Douglas−Kroll−Hess Hamiltonian.[62] Natural bond orbital (NBO) analysis[63] was performed using Gaussian09; Atoms-in-Molecules (AIM) analysis used AIMAll.[64] Topological analysis of the electronic density (ρ) is based upon those points where the gradient of the density, $\nabla\rho$, vanishes.[65] In this work, we consider points where one curvature (in the internuclear direction) is positive and two (perpendicular to the bond direction) are negative, termed (3, −1) or bond critical points. Properties evaluated at such points characterize the bonding interactions present. An electron density (ρ) of 0.2 a.u. or greater typically signifies a covalent bond and less than 0.1 a.u. indicates closed shell (ionic, van der Waals, etc.). Integrated properties of atoms were checked for numerical accuracy via the basin integral of the Laplacian, which should vanish for properly defined atomic basins (all values 10^{-4} or less) and also by comparison of the sum of all atomic integrals with directly calculated molecular values. Integration of the overlap matrix over atomic basins can be used to derive covalent bond order, as set out by Kar and co-workers.[66]

THF was distilled over potassium or Na/benzophenone, while acetonitrile and CD_3CN were distilled over CaH_2 or P_2O_5 and degassed immediately prior to use. $[Et_4N]_4[U(NCS)_8]$,[67] $[Et_4N][U(NCS)_5(bipy)_2]$,[68] and $[Et_4N]_3[UO_2(NCS)_5]$[69] were made via the literature procedures. Lanthanide salts, cesium chloride, sodium thiocyanate, and tetraalkylammonium chlorides were purchased from Sigma and were of reagent grade. They were used without further purification.

Synthesis of $[Et_4N][Pr(NCS)_4(H_2O)_4]$ (1). $PrCl_3{\cdot}7H_2O$ (0.093 g, 0.25 mmol) was dissolved in a 15 mL of acetonitrile−water mixture (4:1, v/v). Then 5 mL of aqueous solution of sodium thiocyanate (0.152 g, 2 mmol) and 10 mL of acetonitrile−water mixture (4:1, v/v) containing tetraethylammonium chloride (0.017 g, 0.10 mmol) solution were added to the metal solution, stirred for 30 min, and then allowed to stand for a week. Light-green colored X-ray quality single crystals of the complex **1** appeared at the bottom of the vessel. Yield = 0.103 g (72%).

Complexes **2**−**5** were obtained from a similar procedure to that of **1**, except that the metal salts $TbCl_3{\cdot}6H_2O$, $DyCl_3{\cdot}6H_2O$, $HoCl_3{\cdot}6H_2O$, and $YbCl_3{\cdot}6H_2O$ (0.093 g (70%), 0.094 g (62%), 0.095 g (75%), and 0.097 g (67%), respectively, with each 0.25 mmol Ln halide) was used instead of praseodymium chloride.

Synthesis of $Cs_5[Nd(NCS)_8]$ (6). Hydrated $NdCl_3$ (0.094 g, 0.20 mmol) was dissolved in a 15 mL of acetonitrile−water mixture (4:1, v/v). Then 5 mL of aqueous solution of sodium thiocyanate (0.122 g, 1.6 mmol) and 10 mL of acetonitrile−water mixture (4:1, v/v) containing cesium chloride (0.168 g, 1.0 mmol) solution were added to the metal solution, stirred for 30 min, and then allowed to stand. Very light-green colored X-ray quality single crystals of the complex appeared at the bottom of the vessel after 1 week.

Synthesis of $[Me_4N]_4[Th(NCS)_7(NO_3)]{\cdot}2MeCN$ (7). To a solution of $[Th(NO_3)_4]{\cdot}5H_2O$ (400 mg, 0.70 mmol) in acetonitrile (30 cm^3) were added NaNCS (455 mg, 5.6 mmol) and Me_4NCl (307 mg, 2.8 mmol). After 1 h of stirring at room temperature, the clear solution was filtered and the solvent was left to evaporate slowly. After 1 week at room temperature, the solution deposited colorless crystals suitable for X-ray diffraction (34.7 mg, 53%). ^1H NMR (400 MHz, CD_3CN): δ 3.17 (s, 12 H, CH_3). $^{13}C\{^1H\}$ NMR (100.64 MHz, CD_3CN): δ 134.8 (NCS), 55.30 (CH_3). IR (ATR, ν/cm^{-1}): 2957 (w, C−H), 2098 (w), 2041 (s, C═N), 1480 (m), 1414 (w), 1365 (w), 1284 (m, NO_3^-), 1027 (w), 945 (m, C═S), 809 (w), 744 (w). Raman (ν/cm^{-1}): 2928, 2257, 2105, and 2061 and 2045 (C═N), 1456, 1425, 1038, 957, 827, 758. UV−vis (ε, $dm^3\ mol^{-1}\ cm^{-1}$), (298 K, MeCN, ~10^{-5} M): 344 nm (125).

Isolation of Heterocycle 9. A cold (−80 °C) solution of $[Et_4N]_4[U(NCS)_8]$ (0.10 g, 0.8 mmol) in MeCN (30 cm^3) was added to a suspension of KC_8 (0.02 g, 5 mmol) in MeCN (20 cm^3) held at −80 °C dropwise. An immediate color change to dark red then colorlessness was observed. Upon warming slowly to room temperature, the mixture was filtered and concentrated. Placement at −30 °C afforded a few colorless crystals suitable for X-ray diffraction.

Synthesis of $[Et_4N]_4[UO_2Cl_4][CuCl_2]$ (10). To a yellow solution of $[Et_4N]_3[UO_2(NCS)_5]$ (200 mg, 0.21 mmol) in acetonitrile (20 cm^3) was added anhydrous $CuCl_2$ (56.5 mg, 0.46 mmol). After 2 h of stirring at room temperature, a clear-brown solution was formed and this was filtered. Slow evaporation of the solvent deposited yellow and green crystals suitable for X-ray diffraction that were separated by hand. IR (ATR, ν/cm^{-1}): 2989 and 2950 (w, C−H), 1460 (m), 1392 (m), 1308 (w), 1184 (m), 1030 (m), 1006 (m), 916 (s, U═O), 789 (m), 637 (w), 603 (w). Raman (ν/cm^{-1}): 1459, 1060, 887, 832 (U═O), 658, 389, 255, 200. UV−vis (ε, $dm^3\ mol^{-1}\ cm^{-1}$), (298 K, MeCN, 2.78 mM): 1381 nm (7.94), 914 nm (7.00), 460 nm (86.4), 310 nm (381), 256 nm (229).

DOI: 10.1021/acs.inorgchem.7b01560
Inorg. Chem. XXXX, XXX, XXX−XXX

■ ASSOCIATED CONTENT

Supporting Information

The Supporting Information is available free of charge on the ACS Publications website at DOI: 10.1021/acs.inorgchem.7b01560.

Full refinement data, spectroscopic data, pXRD, a discussion of the mechanism of formation of the heterocyclic product, and the structure and spectroscopic data for **10** (PDF)

Accession Codes

CCDC 1554951−1554959 and 1574079 contain the supplementary crystallographic data for this paper. These data can be obtained free of charge via www.ccdc.cam.ac.uk/data_request/cif, or by emailing data_request@ccdc.cam.ac.uk, or by contacting The Cambridge Crystallographic Data Centre, 12 Union Road, Cambridge CB2 1EZ, UK; fax: +44 1223 336033.

■ AUTHOR INFORMATION

Corresponding Authors

*R.J.B.: tel, +353-1-8963501; E-mail, bakerrj@tcd.ie.
*F.H.: tel, +44-118-3787695; E-mail, f.hartl@reading.ac.uk.

ORCID

Robert J. Baker: 0000-0003-1416-8659

Present Address

‖S.B.: Department of Chemistry, Katwa College, Katwa, West Bengal 713130, India.

Author Contributions

The manuscript was written through contributions of all authors. All authors have given approval to the final version of the manuscript.

Notes

The authors declare no competing financial interest.

■ ACKNOWLEDGMENTS

We thank the Irish Research Council for funding this work via a Government of Ireland Postdoctoral Fellowship (S.B.) and TCD (S.N.). The University of Reading is thanked for a continued support of the Reading Spectroelectrochemistry laboratory (project D14-015).

■ REFERENCES

(1) (a) Magill, J.; Berthou, V.; Haas, D.; Galy, J.; Schenkel, R.; Wiese, H. W.; Heusener, G.; Tommasi, J.; Youinou, G. Impact limits of partitioning and transmutation scenarios on the radiotoxicity of actinides in radioactive waste. *Nucl. Energy* **2003**, *42*, 263−277. (b) *Potential Benefits and Impacts of Advanced Nuclear Fuel Cycles with Actinide Partitioning and Transmutation*; NEA no. 6894; OECD, Nuclear Energy Agency (NEA): Paris, 2011;. (c) Salvatores, M.; Palmiotti, G. Radioactive waste partitioning and transmutation within advanced fuel cycles: Achievements and challenges. *Prog. Part. Nucl. Phys.* **2011**, *66*, 144−166.

(2) (a) Edwards, A. C.; Mocilac, P.; Geist, A.; Harwood, L. M.; Sharrad, C. A.; Burton, N. A.; Whitehead, R. C.; Denecke, M. A. Hydrophilic 2,9-bis-triazolyl-1,10-phenanthroline ligands enable selective Am(III) separation: a step further towards sustainable nuclear energy. *Chem. Commun.* **2017**, *53*, 5001−5004. (b) Edwards, A. C.; Wagner, C.; Geist, A.; Burton, N. A.; Sharrad, C. A.; Adams, R. W.; Pritchard, R. G.; Panak, P. J.; Whitehead, R. C.; Harwood, L. M. Exploring electronic effects on the partitioning of actinides(III) from lanthanides(III) using functionalised bis-triazinyl phenanthroline ligands. *Dalton Trans.* **2016**, *45*, 18102−18112. (c) Lewis, F. W.; Harwood, L. M.; Hudson, M. J.; Geist, A.; Kozhevnikov, V. N.; Distler, P.; John, J. Hydrophilic sulfonated bis-1,2,4-triazine ligands are highly effective reagents for separating actinides(III) from lanthanides(III) via selective formation of aqueous actinide complexes. *Chem. Sci.* **2015**, *6*, 4812−4821. (d) Afsar, A.; Harwood, L. M.; Hudson, M. J.; Westwood, J.; Geist, A. Effective separation of the actinides Am(III) and Cm(III) by electronic modulation of bis-(1,2,4-triazin-3-yl)phenanthrolines. *Chem. Commun.* **2015**, *51*, 5860−5863. (e) Lewis, F. W.; Harwood, L. M.; Hudson, M. J.; Drew, M. G. B.; Hubscher-Bruder, V.; Videva, V.; Arnaud-Neu, F.; Stamberg, K.; Vyas, S. BTBPs versus BTPhens: Some Reasons for Their Differences in Properties Concerning the Partitioning of Minor Actinides and the Advantages of BTPhens. *Inorg. Chem.* **2013**, *52*, 4993−5005. (f) Hudson, M. J.; Harwood, L. M.; Laventine, D. M.; Lewis, F. W. Use of Soft Heterocyclic N-Donor Ligands To Separate Actinides and Lanthanides. *Inorg. Chem.* **2013**, *52*, 3414−3428 and references therein..

(3) Panak, P. J.; Geist, A. Complexation and Extraction of Trivalent Actinides and Lanthanides by Triazinylpyridine N-Donor Ligands. *Chem. Rev.* **2013**, *113*, 1199−1236.

(4) (a) Fryer-Kanssen, I.; Austin, J.; Kerridge, A. Topological Study of Bonding in Aquo and Bis(triazinyl)pyridine Complexes of Trivalent Lanthanides and Actinides: Does Covalency Imply Stability? *Inorg. Chem.* **2016**, *55*, 10034−10042. and references therein; (b) Neidig, M. L.; Clark, D. L.; Martin, R. L. Covalency in f-element complexes. *Coord. Chem. Rev.* **2013**, *257*, 394−406.

(5) (a) Rivière, C.; Nierlich, M.; Ephritikhine, M.; Madic, C. Complexation Studies of Iodides of Trivalent Uranium and Lanthanides (Ce and Nd) with 2,2′-Bipyridine in Anhydrous Pyridine Solutions. *Inorg. Chem.* **2001**, *40*, 4428−4435. (b) Berthet, J. − C.; Rivière, C.; Miquel, Y.; Nierlich, M.; Madic, C.; Ephritikhine, M. Selective complexation of uranium(III) over cerium(III) and neodymium(III) by 2,2′:6′,2″-terpyridine - x-ray crystallographic evidence for uranium-to-ligand π back-bonding. *Eur. J. Inorg. Chem.* **2002**, *2002*, 1439−1446. (c) Berthet, J. − C.; Miquel, Y.; Iveson, P. B.; Nierlich, M.; Thuéry, P.; Madic, C.; Ephritikhine, M. The affinity and selectivity of terdentate nitrogen ligands towards trivalent lanthanide and uranium ions viewed from the crystal structures of the 1:3 complexes. *J. Chem. Soc., Dalton Trans.* **2002**, 3265−3272. (d) Mazzanti, M.; Wietzke, R.; Pécaut, J.; Latour, J.-M.; Maldivi, P.; Remy, M. Structural and Density Functional Studies of Uranium(III) and Lanthanum(III) Complexes with a Neutral Tripodal N-Donor Ligand Suggesting the Presence of a U-N Back-Bonding Interaction. *Inorg. Chem.* **2002**, *41*, 2389−2399.

(6) (a) Borkowski, M.; Lis, S.; Siekierski, S. Complexation of f electron (3+) ions with pseudohalide ligands. *J. Alloys Compd.* **1998**, *275−277*, 754−758. (b) Borkowski, M.; Krejzler, J.; Siekierski, S. The effect of the pseudohalide ligand on solvent extraction of trivalent lanthanides, yttrium and americium by tri-n-butyl phosphate. *Radiochim. Acta* **1994**, *65*, 99−103. (c) Khopkar, P. K.; Mathur, J. N. Complexing of californium(III) and other trivalent actinides by inorganic ligands. *J. Inorg. Nucl. Chem.* **1980**, *42*, 109−113. (d) Khopkar, P. K.; Mathur, J. N. Thiocyanate complexing of trivalent actinides and lanthanides. *J. Inorg. Nucl. Chem.* **1974**, *36*, 3819−3825. (e) Chiarizia, R.; Danesi, P. R.; Scibona, G.; Magon, L. Liquid anion exchange of thiocyanate-nitrate actinide and lanthanide complexes. *J. Inorg. Nucl. Chem.* **1973**, *35*, 3595−3604. (f) Khopkar, P. K.; Narayanankutty, P. Effect of ionic media on the stability constants of chloride, nitrate and thiocyanate complexes of americium(III) and europium(III). *J. Inorg. Nucl. Chem.* **1971**, *33*, 495−502. (g) Moore, F. L. New approach to separation of trivalent actinide elements from lanthanide elements-selective liquid-liquid extraction with tricaprylmethylammonium thiocyanate. *Anal. Chem.* **1964**, *36*, 2158−2162.

(7) Srncik, M.; Kogelnig, D.; Stojanovic, A.; Korner, W.; Krachler, R.; Wallner, G. Uranium extraction from aqueous solutions by ionic liquids. *Appl. Radiat. Isot.* **2009**, *67*, 2146−2149.

(8) Petrosyants, S. P. Coordination compounds of rare-earth metal thiocyanates. *Russ. J. Coord. Chem.* **2015**, *41*, 715−729.

(9) Mullica, D. F.; Farmer, J. M.; Kautz, J. A. Synthesis and structural investigation of tris(tetra-n-butylammonium)-diisothiocyanatotetranitratocerinate(III). *Inorg. Chem. Commun.* **1998**, *1*, 217−221.

DOI: 10.1021/acs.inorgchem.7b01560
Inorg. Chem. XXXX, XXX, XXX−XXX

(10) Farmer, J. M.; Kautz, J. A.; Kwon, H. S.; Mullica, D. F. Syntheses, characterization, and structural analyses of several f-block isothiocyanatonitrato complexes. *J. Chem. Crystallogr.* **2000**, *30*, 301−309.
(11) Petrosyants, S.; Dobrokhotova, Z.; Ilyukhin, A.; Efimov, N.; Mikhlina, Y.; Novototsev, V. Europium and terbium thiocyanates: Syntheses, crystal structures, luminescence and magnetic properties. *Inorg. Chim. Acta* **2015**, *434*, 41−50.
(12) Mullica, D. F.; Bonilla, B. M.; David, M. C.; Farmer, J. M.; Kautz, J. A. Synthesis, characterization, and structural analyses of three high-coordination tetra-n-butylammonium lanthanide(III) complexes. *Inorg. Chim. Acta* **1999**, *292*, 137−143.
(13) Gröb, T.; Harms, K.; Dehnicke, K. Kristallstruktur des Isothiocyanato-Komplexes $[Ph_3PNH_2(OEt_2)][Sm(NCS)_4(DME)_2]$. *Z. Anorg. Allg. Chem.* **2001**, *627*, 125−127.
(14) Matsumura, N.; Takeuchi, T.; Ouchi, A. The syntheses, crystal and molecular structures, and thermal properties of tetramethylammonium [octakis(isothiocyanato)lanthanoidates(III)].2(benzene), $[(CH_3)_4N]_5[M(NCS)_8].2C_6H_6$ (M = La, Ce, Pr, Nd, Sm, Eu, Gd, Tb, Dy). *Bull. Chem. Soc. Jpn.* **1990**, *63*, 620−622.
(15) Nockemann, P.; Thijs, B.; Postelmans, N.; Van Hecke, K.; Van Meervelt, L.; Binnemans, K. Anionic Rare-Earth Thiocyanate Complexes as Building Blocks for Low-Melting Metal-Containing Ionic Liquids. *J. Am. Chem. Soc.* **2006**, *128*, 13658−13659.
(16) Mallick, B.; Balke, B.; Felser, C.; Mudring, A.-V. Dysprosium room-temperature ionic liquids with strong luminescence and response to magnetic fields. *Angew. Chem., Int. Ed.* **2008**, *47*, 7635−7638.
(17) Carter, T. J.; Wilson, R. E. Coordination Chemistry of Homoleptic Actinide(IV)-Thiocyanate Complexes. *Chem. - Eur. J.* **2015**, *21*, 15575−15582.
(18) Matsumoto, F.; Matsumura, N.; Ouchi, A. Syntheses and crystal and molecular structures of tetramethylammonium [aquamethanolhexakis(isothiocyanato)lanthanoidates(III)], $[(CH_3)_4N]_3[M(NCS)_6(CH_3OH)(H_2O)]$ (M = La, Ce, Pr, Nd, Sm, Eu, Gd, Tb, Dy, Er), and tetramethylammonium [heptakis-(isothiocyanato)lanthanoidates(III)], $[(CH_3)_4N]_4[M(NCS)_7]$ (M = Dy, Er, Yb). *Bull. Chem. Soc. Jpn.* **1989**, *62*, 1809−1816.
(19) Ouchi, A. The Crystal and Molecular Structures of Tetraethylammonium [Tetraaquatetrakis(isothiocyanato)neodymate-(III) and europate(III)], $[(C_2H_5)_4N][M(NCS)_4(H_2O)_4]$, (M = Nd, Eu). *Bull. Chem. Soc. Jpn.* **1989**, *62*, 2431−2433.
(20) Lozano-Rodriguez, M. J.; Copping, R.; Petit, S.; Solari, P. L.; Guilbaud, P.; Mustre de Leon, J.; Den Auwer, C. Crystal structure versus solution for two new lutetium thiocyanato complexes. *New J. Chem.* **2011**, *35*, 2755−2765.
(21) Matsumoto, F.; Takeuchi, T.; Ouchi, A. The crystal and molecular structures of tetraethylammonium [heptakis-(isothiocyanato)lanthanate(III) and -praseodymate(III)].benzene, $[(C_2H_5)_4N]_4[M(SCN)_7].C_6H_6$ (M = La, Pr), in a unicapped trigonal prism geometry. *Bull. Chem. Soc. Jpn.* **1989**, *62*, 2078−2080.
(22) (a) Savard, D.; Leznoff, D. B. Synthesis, structure and light scattering properties of tetraalkylammonium metal isothiocyanate salts. *Dalton Trans.* **2013**, *42*, 14982−14991. (b) Thompson, L. C.; Radonovich, L. J. Structure of tris (tetrabutylammonium) hexaisothiocyanatoerbate(III). *Acta Crystallogr., Sect. C: Cryst. Struct. Commun.* **1990**, *46*, 1618−1621. (c) Mullica, D. F.; Kautz, J. A.; Sappenfield, E. L. Structural analysis of tris(tetra-n-butylammonium) hexakisisothiocyanatolutetate(III). *Inorg. Chim. Acta* **1997**, *256*, 115−119. (d) Martin, J. L.; Thompson, L. C.; Radonovich, L. J.; Glick, M. D. Synthesis and structure of the six-coordinate hexaisothiocyanatolanthanide(III) complexes. *J. Am. Chem. Soc.* **1968**, *90*, 4493−4494.
(23) Arai, H.; Suzuki, Y.; Matsumura, N.; Takeuchi, T.; Ouchi, A. Syntheses, and crystal and molecular structures of tetraethylammonium [hexakis(isothiocyanato)lanthanoidates(III)] including aromatic hydrocarbon or halohydrocarbon: $[(C_2H_5)_4N]_3[M(NCS)_6]\cdot G$ (M = erbium, ytterbium; G = benzene, fluorobenzene, toluene, or chlorobenzene). *Bull. Chem. Soc. Jpn.* **1989**, *62*, 2530−2535.
(24) Lozano-Rodriguez, M. J.; Thuery, P.; Petit, S.; Copping, R.; Mustre de Leon, J.; Den Auwer, C. Tris(tetra-butyl-ammonium) tris-(nitrato-κ^2O,O′)tetra-kis-(thio-cyanato-κN)thorium(IV). *Acta Crystallogr., Sect. E: Struct. Rep. Online* **2011**, *67*, m487.
(25) Charpin, P.; Lance, M.; Navaza, A. Structure of a cubic form of tetra-ethylammonium octakis-(thio-cyanato-N)thorate(IV), $[N(C_2H_5)_4]_4[Th(NCS)_8]$. *Acta Crystallogr., Sect. C: Cryst. Struct. Commun.* **1983**, *39*, 190−192.
(26) Countryman, R.; McDonald, W. S. The crystal structure of tetraethylammonium octathiocyanato-n-uranate(IV), $[(C_2H_5)_4N]_4[U(NCS)_8]$: An example of cubical 8-coordination. *J. Inorg. Nucl. Chem.* **1971**, *33*, 2213−2220.
(27) Budantseva, N. A.; Andreev, G. B.; Fedoseev, A. M.; Antipin, M. Y. Tetramethylammonium Neptunium(IV) Isothiocyanate $[N(CH_3)_4]_4[Np(NCS)_8]$. *Radiochemistry* **2003**, *45*, 335−338.
(28) Bagnall, K. W.; Benetollo, F.; Forsellini, E.; Bombieri, G. The crystal and molecular structures of the N,N′-diisopropylbutyramide (DIPIBA) and N,N-dicyclohexylacetamide (DCA) complexes $[Th(NCS)_4(DIPIBA)_3]$ and $[Th(NCS)_2Cl_2(DCA)_3]$. *Polyhedron* **1992**, *11*, 1765−1770.
(29) Cotton, S. A.; Franckevicius, V.; How, R. E.; Ahrens, B.; Ooi, L. L.; Mahon, M. F.; Raithby, P. R.; Teat, S. J. Synthesis of complexes of 2,2′:6′,2″-terpyridine and 1,10-phenanthroline with lanthanide thiocyanates; the molecular structures of $[Ln(terpy)_2(NCS)_3]$ (Ln = Pr, Nd), $[Nd(terpy)_2(NCS)_3]\cdot 2EtOH$ and $[Ln(phen)_3(NCS)_3]\cdot EtOH$ (Ln = Pr, Nd). *Polyhedron* **2003**, *22*, 1489−1497.
(30) Hashem, E.; Platts, J. A.; Hartl, F.; Lorusso, G.; Evangelisti, M.; Schulzke, C.; Baker, R. J. Thiocyanate Complexes of Uranium in Multiple Oxidation States: A Combined Structural, Magnetic, Spectroscopic, Spectroelectrochemical, and Theoretical Study. *Inorg. Chem.* **2014**, *53*, 8624−8637.
(31) Hashem, E.; Lorusso, G.; Evangelisti, M.; McCabe, T.; Schulzke, C.; Platts, J. A.; Baker, R. J. Fingerprinting the oxidation state of U(IV) by emission spectroscopy. *Dalton Trans.* **2013**, *42*, 14677−14680.
(32) (a) Reddi, R.; Singarapu, K. K.; Pal, D.; Addlagatta, A. The unique functional role of the C−H···S hydrogen bond in the substrate specificity and enzyme catalysis of type 1 methionine aminopeptidase. *Mol. BioSyst.* **2016**, *12*, 2408−2416. (b) Wei, K. J.; Ni, J.; Xie, Y. S.; Liu, Q. L. Solvent-induced 1- and 2-D Cd(II) coordination polymers based on a bent polypyridyl ligand. *Inorg. Chem. Commun.* **2007**, *10*, 279−282. (c) Zhou, H. P.; Zhu, Y. M.; Chen, J. J.; Hu, Z. J.; Wu, J. Y.; Xie, Y.; Jiang, M. H.; Tao, X. T.; Tian, Y. P. A new ligand for the formation of a 3D structure by significant C−H···S hydrogen bonds and $\pi-\pi$ interactions. *Inorg. Chem. Commun.* **2006**, *9*, 90−92. (d) Allen, F. H.; Bird, C. M.; Rowland, R. S.; Raithby, P. R. Hydrogen-Bond Acceptor and Donor Properties of Divalent Sulfur (Y—S–Z and R—S–H). *Acta Crystallogr., Sect. B: Struct. Sci.* **1997**, *53*, 696−701. (e) Desiraju, G. R.; Steiner, T. *The Weak Hydrogen Bond in Structural Chemistry and Biology*; Oxford University Press, 1999.
(33) La Pierre, H. S.; Heinemann, F. W.; Meyer, K. Well-defined molecular uranium(III) chloride complexes. *Chem. Commun.* **2014**, *50*, 3962−3964.
(34) Antunes, M. A.; Dias, M.; Monteiro, B.; Domingos, A.; Santos, I. C.; Marques, N. Synthesis and reactivity of uranium(IV) amide complexes supported by a triamidotriazacyclononane ligand. *Dalton Trans.* **2006**, 3368−3374.
(35) Avens, L. R.; Barnhart, D. M.; Burns, C. J.; McKee, S. D. Uranium-Mediated Ring Opening of Tetrahydrofuran. Crystal Structure of $UI_2(OCH_2CH_2CH_2CH_2I)_2(Ph_3PO)_2$. *Inorg. Chem.* **1996**, *35*, 537−539.
(36) Larch, C. P.; Cloke, F. G. N.; Hitchcock, P. B. Activation and reduction of diethyl ether by low valent uranium: formation of the trimetallic, mixed valence uranium oxo species $[U(Cp^{RR'})(\mu\text{-}I)_2]_3(\mu^3\text{-}O)$ ($Cp^{RR'}$ = C_5Me_5, C_5Me_4H, $C_5H_4SiMe_3$). *Chem. Commun.* **2008**, 82−84.
(37) Evans, W. J.; Miller, K. A.; Ziller, J. W. Reductive Coupling of Acetonitrile by Uranium and Thorium Hydride Complexes To Give Cyanopentadienyl Dianion (C6N3H7)2−. *Angew. Chem., Int. Ed.* **2008**, *47*, 589−592.

DOI: 10.1021/acs.inorgchem.7b01560
Inorg. Chem. XXXX, XXX, XXX−XXX

(38) See for example the reduction of methylene blue: Pande, S.; Ghosh, S. K.; Nath, S.; Praharaj, S.; Jana, S.; Panigrahi, S.; Basu, S.; Pal, T. Reduction of methylene blue by thiocyanate: Kinetic and thermodynamic aspects. *J. Colloid Interface Sci.* **2006**, *299*, 421−427.
(39) For recent review on transition metal bipy complexes see: Scarborough, C. C.; Wieghardt, K. Electronic Structure of 2,2′-Bipyridine Organotransition-Metal Complexes. Establishing the Ligand Oxidation Level by Density Functional Theoretical Calculations. *Inorg. Chem.* **2011**, *50*, 9773−9793.
(40) (a) Coutinho, J. T.; Antunes, M. A.; Pereira, L. C. J.; Marcalo, J.; Almeida, M. Zero-field slow magnetic relaxation in a uranium(III) complex with a radical ligand. *Chem. Commun.* **2014**, *50*, 10262−10264. (b) Antunes, M. A.; Pereira, L. C. J.; Santos, I. C.; Mazzanti, M.; Marcalo, J.; Almeida, M. $[U(Tp^{Me2})_2(bipy)]^+$: A Cationic Uranium(III) Complex with Single-Molecule-Magnet Behavior. *Inorg. Chem.* **2011**, *50*, 9915−9917. (c) Kraft, S. J.; Fanwick, P. E.; Bart, S. C. Synthesis and Characterization of a Uranium(III) Complex Containing a Redox-Active 2,2′-Bipyridine Ligand. *Inorg. Chem.* **2010**, *49*, 1103−1110.
(41) (a) Rosenzweig, M. W.; Heinemann, F. W.; Maron, L.; Meyer, K. Molecular and Electronic Structures of Eight-Coordinate Uranium Bipyridine Complexes: A Rare Example of a $Bipy^{2-}$ Ligand Coordinated to a U^{4+} Ion. *Inorg. Chem.* **2017**, *56*, 2792−2800. (b) Diaconescu, P. L.; Cummins, C. C. Radical anionic versus neutral 2,2′-bipyridyl coordination in uranium complexes supported by amide and ketimide ligands. *Dalton Trans.* **2015**, *44*, 2676−2683. (c) Takase, M. K.; Fang, M.; Ziller, J. W.; Furche, F.; Evans, W. J. Reduction chemistry of the mixed ligand metallocene $[(C_5Me_5)(C_8H_8)U]_2(\mu\text{-}C_8H_8)$ with bipyridines. *Inorg. Chim. Acta* **2010**, *364*, 167−171. (d) Ren, W.; Lukens, W. W.; Zi, G.; Maron, L.; Walter, M. D. Is the bipyridyl thorium metallocene a low-valent thorium complex? A combined experimental and computational study. *Chem. Sci.* **2013**, *4*, 1168−1174.
(42) Fortier, S.; Veleta, J.; Pialat, A.; Le Roy, J.; Ghiassi, K. B.; Olmstead, M. M.; Metta-Magana, A.; Murugesu, M.; Villagran, D. $[U(bipy)_4]$: A Mistaken Case of U^0? *Chem. - Eur. J.* **2016**, *22*, 1931−1936.
(43) Dissociation of NCS^- ions under SEC conditions have previously been noted: Kamper, S.; Paretzki, A.; Fiedler, J.; Zalis, S.; Kaim, W. Solar Cell Sensitizer Models $[Ru(bpy\text{-}R)_2(NCS)_2]$ Probed by Spectroelectrochemistry. *Inorg. Chem.* **2012**, *51*, 2097−2104.
(44) Grenthe, I.; Drożdżyński, J.; Fujino, T.; Buck, E. C.; Albrecht-Schmitt, T. A.; Wolf, S. F. *The Chemistry of the Actinides and Transactinides*, 4th ed.; Morss, L. R.; Edelstein, N. M.; Fuger, J. Springer: Dordrect, The Netherlands, 2010; Chapter 5.
(45) (a) Collado, S.; Laca, A.; Díaz, M. Catalytic wet oxidation of thiocyanate with homogeneous copper(II) sulphate catalyst. *J. Hazard. Mater.* **2010**, *177*, 183−189. (b) Kirschenbaum, L. J.; Sun, Y. Reduction of the Tetrahydroxoargentate(111) Ion by Thiocyanate in Aqueous Alkaline Media. *Inorg. Chem.* **1991**, *30*, 2360−2365.
(46) (a) Jung, J.; Atanasov, M.; Neese, F. Ab Initio Ligand-Field Theory Analysisand Covalency Trends in Actinide and Lanthanide Free Ions and Octahedral Complexes. *Inorg. Chem.* **2017**, *56*, 8802−8816. (b) Kerridge, A. Quantification of f-element covalency through analysis of the electron density: insights from simulation. *Chem. Commun.* **2017**, *53*, 6685−6695. (c) Dognon, J.-P. Electronic structure theory to decipher the chemical bonding in actinide systems. *Coord. Chem. Rev.* **2017**, *344*, 150−162.
(47) Beekmeyer, R.; Kerridge, A. Assessing Covalency in Cerium and Uranium Hexachlorides: A Correlated Wavefunction and Density Functional Theory Study. *Inorganics* **2015**, *3*, 482−499.
(48) Bruker (2012−2015) APEX v2012.12-0 to v2015.9-0 ; Bruker AXS Inc., Madison, Wisconsin, USA.
(49) Sheldrick, G. M. SHELXT − Integrated space-group and crystal-structure determination. *Acta Crystallogr., Sect. A: Found. Adv.* **2015**, *71*, 3−8.
(50) Sheldrick, G. M. A short history of SHELX. *Acta Crystallogr., Sect. A: Found. Crystallogr.* **2008**, *64*, 112−122.
(51) Dolomanov, O. V.; Bourhis, L. J.; Gildea, R. J.; Howard, J. A. K.; Puschmann, H. OLEX2: a complete structure solution, refinement and analysis program. *J. Appl. Crystallogr.* **2009**, *42*, 339−341.
(52) Sheldrick, G. M. *SADABS*; Bruker AXS Inc., Madison, WI, 2014; University of Göttingen, Germany.
(53) Momma, K.; Izumi, F. VESTA 3 for three-dimensional visualization of crystal, volumetric and morphology data. *J. Appl. Crystallogr.* **2011**, *44*, 1272−1276.
(54) Krejčík, M.; Daněk, M.; Hartl, F. Simple construction of an infrared optically transparent thin-layer electrochemical cell: Applications to the redox reactions of ferrocene, $Mn_2(CO)_{10}$ and $Mn(CO)_3$(3,5-di-t-butyl-catecholate)$^-$. *J. Electroanal. Chem. Interfacial Electrochem.* **1991**, *317*, 179−187.
(55) (a) Becke, A. D. Density-functional exchange-energy approximation with correct asymptotic behavior. *Phys. Rev. A: At., Mol., Opt. Phys.* **1988**, *38*, 3098−3100. (b) Perdew, J. P. Density-functional approximation for the correlation energy of the inhomogeneous electron gas. *Phys. Rev. B: Condens. Matter Mater. Phys.* **1986**, *33*, 8822−8824.
(56) Weigend, F.; Ahlrichs, R. Balanced basis sets of split valence, triple zeta valence and quadruple zeta valence quality for H to Rn: Design and assessment of accuracy. *Phys. Chem. Chem. Phys.* **2005**, *7*, 3297−3305.
(57) Turbomole v5.10 Ahlrichs, R.; Baer, M.; Haeser, M.; Horn, H.; Koelmel, C. *Chem. Phys. Lett.* **1989**, *162*, 165−169.
(58) Frisch, M. J.; Trucks, G. W.; Schlegel, H. B.; Scuseria, G. E.; Robb, M. A.; Cheeseman, J. R.; Scalmani, G.; Barone, V.; Mennucci, B.; Petersson, G. A.; Nakatsuji, H.; Caricato, M.; Li, X.; Hratchian, H. P.; Izmaylov, A. F.; Bloino, J.; Zheng, G.; Sonnenberg, J. L.; Hada, M.; Ehara, M.; Toyota, K.; Fukuda, R.; Hasegawa, J.; Ishida, M.; Nakajima, T.; Honda, Y.; Kitao, O.; Nakai, H.; Vreven, T.; Montgomery, J. A., Jr.; Peralta, J. E.; Ogliaro, F.; Bearpark, M.; Heyd, J. J.; Brothers, E.; Kudin, K. N.; Staroverov, V. N.; Keith, T.; Kobayashi, R.; Normand, J.; Raghavachari, K.; Rendell, A.; Burant, J. C.; Iyengar, S. S.; Tomasi, J.; Cossi, M.; Rega, N.; Millam, J. M.; Klene, M.; Knox, J. E.; Cross, J. B.; Bakken, V.; Adamo, C.; Jaramillo, J.; Gomperts, R.; Stratmann, R. E.; Yazyev, O.; Austin, A. J.; Cammi, R.; Pomelli, C.; Ochterski, J. W.; Martin, R. L.; Morokuma, K.; Zakrzewski, V. G.; Voth, G. A.; Salvador, P.; Dannenberg, J. J.; Dapprich, S.; Daniels, A. D.; Farkas, O.; Foresman, J. B.; Ortiz, J. V.; Cioslowski, J.; Fox, D. J., *Gaussian 09*, revision B.01; Gaussian, Inc.: Wallingford CT, 2010.
(59) (a) Becke, A. D. Density-functional thermochemistry. III. The role of exact exchange. *J. Chem. Phys.* **1993**, *98*, 5648−5652. (b) Lee, C.; Yang, W.; Parr, R. G. Development of the Colle-Salvetti correlation-energy formula into a functional of the electron density. *Phys. Rev. B: Condens. Matter Mater. Phys.* **1988**, *37*, 785−789.
(60) Roos, B. O.; Lindh, R.; Malmqvist, P.-Å.; Veryazov, V.; Widmark, P.-O.; Borin, A. C. New Relativistic Atomic Natural Orbital Basis Sets for Lanthanide Atoms with Applications to the Ce Diatom and LuF_3. *J. Phys. Chem. A* **2008**, *112*, 11431−11435.
(61) (a) Hehre, W. J.; Ditchfield, R.; Pople, J. A. Self—Consistent Molecular Orbital Methods. XII. Further Extensions of Gaussian—Type Basis Sets for Use in Molecular Orbital Studies of Organic Molecules. *J. Chem. Phys.* **1972**, *56*, 2257−2261. (b) Clark, T.; Chandrasekhar, J.; Spitznagel, G. W.; Schleyer, P. V. R. Efficient diffuse function-augmented basis sets for anion calculations. III. The 3-21+G basis set for first-row elements, Li−F. *J. Comput. Chem.* **1983**, *4*, 294−301. (c) Hariharan, P. C.; Pople, J. A. The influence of polarization functions on molecular orbital hydrogenation energies. *Theoret. Chimica Acta* **1973**, *28*, 213−222.
(62) Jansen, G.; Hess, B. A. Revision of the Douglas-Kroll transformation. *Phys. Rev. A: At., Mol., Opt. Phys.* **1989**, *39*, 6016−6017 and references cited therein..
(63) Reed, A. E.; Weinhold, F. Natural localized molecular orbitals. *J. Chem. Phys.* **1985**, *83*, 1736−1740.
(64) Keith, T. *AIMAll*, version 17.01.25; 2017; http://aim.tkgristmill.com.
(65) Bader, R. F. W. *Atoms in Molecules—A Quantum Theory*; Oxford University Press; Oxford, UK, 1990.

DOI: 10.1021/acs.inorgchem.7b01560
Inorg. Chem. XXXX, XXX, XXX−XXX

(66) Kar, T.; Angyan, J. G.; Sannigrahi, A. B. Comparison of ab Initio Hartree−Fock and Kohn−Sham Orbitals in the Calculation of Atomic Charge, Bond Index, and Valence. *J. Phys. Chem. A* **2000**, *104*, 9953−9963.
(67) Bagnall, K. W.; Brown, D.; Colton, R. The magnetic and spectral properties of some uranium(IV) complexes. *J. Chem. Soc.* **1964**, 2527−2530.
(68) Wiley, R. O.; Von Dreele, R. B.; Brown, T. M. Synthesis, characterization, and molecular structure of tetraethylammonium pentakis(isothiocyanato)bis(2,2′-bipyridine)uranate(IV). *Inorg. Chem.* **1980**, *19*, 3351−3356.
(69) Rowland, C. E.; Kanatzidis, M. G.; Soderholm, L. Tetraalkylammonium Uranyl Isothiocyanates. *Inorg. Chem.* **2012**, *51*, 11798−11804.

DOI: 10.1021/acs.inorgchem.7b01560
Inorg. Chem. XXXX, XXX, XXX−XXX